Cellular/Molecular

The DEP Domain Determines Subcellular Targeting of the GTPase Activating Protein RGS9 *In Vivo*

Kirill A. Martemyanov,[1] Polina V. Lishko,[1] Nidia Calero,[2] Gabor Keresztes,[3] Maxim Sokolov,[1] Katherine J. Strissel,[1] Ilya B. Leskov,[1] Johnathan A. Hopp,[1] Alexander V. Kolesnikov,[1] Ching-Kang Chen,[4] Janis Lem,[5] Stefan Heller,[3] Marie E. Burns,[2] and Vadim Y. Arshavsky[1]

[1]Howe Laboratory of Ophthalmology, Harvard Medical School and the Massachusetts Eye and Ear Infirmary, Boston, Massachusetts 02114, [2]Center for Neuroscience and Department of Psychiatry, University of California Davis, Davis, California 95616, [3]Department of Otology and Laryngology, Harvard Medical School and Eaton Peabody Laboratory at the Massachusetts Eye and Ear Infirmary, Boston, Massachusetts 02114, [4]Department of Ophthalmology and Visual Sciences, University of Utah, Salt Lake City, Utah 84112, and [5]Molecular Cardiology Research Institute, Department of Ophthalmology, and Program in Genetics, Tufts University School of Medicine and New England Medical Center, Boston, Massachusetts 02111

DEP (for Disheveled, EGL-10, Pleckstrin) homology domains are present in numerous signaling proteins, including many in the nervous system, but their function remains mostly elusive. We report that the DEP domain of a photoreceptor-specific signaling protein, RGS9 (for regulator of G-protein signaling 9), plays an essential role in RGS9 delivery to the intracellular compartment of its functioning, the rod outer segment. We generated a transgenic mouse in which RGS9 was replaced by its mutant lacking the DEP domain. We then used a combination of the quantitative technique of serial tangential sectioning–Western blotting with electrophysiological recordings to demonstrate that mutant RGS9 is expressed in rods in the normal amount but is completely excluded from the outer segments. The delivery of RGS9 to rod outer segments is likely to be mediated by the DEP domain interaction with a transmembrane protein, R9AP (for RGS9 anchoring protein), known to anchor RGS9 on the surface of photoreceptor membranes and to potentiate RGS9 catalytic activity. We show that both of these functions are also abolished as the result of the DEP domain deletion. These findings indicate that a novel function of the DEP domain is to target a signaling protein to a specific compartment of a highly polarized neuron. Interestingly, sequence analysis of R9AP reveals the presence of a conserved R-SNARE (for soluble *N*-ethylmaleimide-sensitive factor attachment protein receptor) motif and a predicted overall structural homology with SNARE proteins involved in vesicular trafficking and fusion. This presents the possibility that DEP domains might serve to target various DEP-containing proteins to the sites of their intracellular action via interactions with the members of extended SNARE protein family.

Key words: **DEP domains; RGS proteins; SNARE proteins; protein targeting; photoreceptors; retina**

Introduction

DEP (for Disheveled, EGL-10, Pleckstrin) homology domains of ~70 amino acids are present in numerous signaling proteins (Ponting and Bork, 1996; Burchett, 2000), including 67 found in the human genome (according to the SMART database). Proteins containing the DEP domain regulate a broad range of cellular functions, from determination of planar cell polarity in early embryonic development (Sokol, 2000) to highly specialized neuronal signaling in photoreceptors of the retina (for review, see Arshavsky et al., 2002). Although DEP domains are often described as being of unknown function, evidence is emerging that several signaling proteins may rely on their DEP domains for membrane association (Axelrod et al., 1998; de Rooij et al., 2000; Hoffman et al., 2000; Hu and Wensel, 2002; Lishko et al., 2002; Patikoglou and Koelle, 2002; Qiao et al., 2002).

Vertebrate photoreceptors provide a unique opportunity to merge biochemical, electrophysiological, and transgenic approaches in pursuit of the functions of the DEP-containing protein RGS9 (for regulator of G-protein signaling). RGS9 is a GTPase-activating protein that sets the duration of the photoreceptor response to light by regulating the lifetime of activated G-protein transducin (He et al., 1998) (for review, see Cowan et al., 2000; Arshavsky et al., 2002). In photoreceptors, RGS9 exists as a constitutive complex with type 5 G-protein β-subunit (Gβ5) (Makino et al., 1999), which is tightly associated with the membranes of photoreceptor outer segments via RGS9 anchor protein (R9AP) (Hu and Wensel, 2002; Lishko et al., 2002). An important property of photoreceptor outer segments is that they contain a set of specific proteins responsible for conducting visual signal transduction and exclude most other cellular proteins. This makes the problem of protein sorting and transporting to the

Received Aug. 6, 2003; revised Sept. 11, 2003; accepted Sept. 12, 2003.

This work was supported by National Institutes of Health (NIH) Grants EY 12859 (V.Y.A.), DC04563 (S.H.), EY14147 (M.E.B.), and EY12008 (J.L.), an American Heart Association award (K.A.M.), Massachusetts Lions Eye Research Fund grants (V.Y.A. and the New England Medical Center, Department of Ophthalmology), a Knights Templar award (M.S.), the E. Matilda Ziegler Foundation Award (M.E.B.), and March of Dimes Birth Defects Foundation Grant 5-FY00-528 (S.H.). The Tufts University–New England Medical Center Transgenic Core Facility was supported by NIH Specialized Center of Research Grant P50HL63494. M.E.B. is an Alfred P. Sloan Research Fellow. V.Y.A. is a recipient of the Jules and Doris Stein Professorship from Research to Prevent Blindness.

Correspondence should be addressed to Dr. Vadim Y. Arshavsky, Department of Ophthalmology, Harvard Medical School, Howe Laboratory–Massachusetts Eye and Ear Infirmary, 243 Charles Street, Boston, MA 02114. E-mail: vadim_arshavsky@meei.harvard.edu.

 0270-6474/03/2310175-07$15.00/0

outer segments one of the central unsolved problems in photoreceptor cell biology (for review, see Sung and Tai, 2000; Williams, 2002).

Here we show that the DEP domain of RGS9 is essential for the delivery of RGS9 to rod outer segments (ROS) *in vivo*. Using transgenic mice that expressed an RGS9 mutant lacking the DEP domain, we found that the mutant transgene protein was expressed in normal amounts but was completely excluded from rod outer segments, resulting in a complete loss of the ability of RGS9 to regulate the duration of the responses to light by the photoreceptors. In contrast, the normal rod outer segment localization of R9AP in these mice was not affected by the mutation. We also show that the deletion of the DEP domain completely abolished the regulation of RGS9 activity by R9AP, consistent with previous reports that the presence of DEP domain is required for RGS9 binding to R9AP (Lishko et al., 2002; Hu et al., 2003). These observations suggest that the DEP domain of RGS9 serves as a "passport," allowing RGS9 delivery to rod outer segments via the interaction with R9AP that has to take place outside the outer segments.

Materials and Methods

Generation of DEP-less transgenic mouse. The DNA region encoding RGS9ΔDEP (amino acids 112–484) was amplified by PCR from RGS9 cDNA using the *Sal*I-containing upstream primer 5′-GATCGTCGACATGCAGCAGTGGCCAGCTGAAGAC-3′ and the *Bam*HI-containing downstream primer 5′- ACGGGATCCTCATTTAGGAGGCAGCTCCTTTT-3′. PCR fragment was cloned into rod-specific mammalian expression vector provided by S. Tsang (University of California Los Angeles, Los Angeles, CA) (Tsang et al., 1998). In the resulting plasmid, the open reading frame of RGS9ΔDEP was located under the control of a 4.4 kb mouse opsin promoter region and supplied with the polyadenylation signal of the mouse protamine gene (Lem et al., 1991). The construct was injected into the pronuclei of oocytes from superovulated females of BDF1 strain (F1 of C57BL/6 × DBA/2; Charles River Laboratories, Wilmington, MA). The transgene integration was determined by Southern blot and PCR analyses of tail DNA. To establish the transgenic line, founders were first crossed with C57BL/6 animals and then with RGS9−/− mice (Chen et al., 2000). To obtain the line in which RGS9ΔDEP is expressed on the RGS9 knock-out background (RGS9−/−), hemizygous mice (RGS9−/+) stably expressing the transgene were backcrossed with the RGS9−/− line. The resulting transgenic animal contained genetic contributions from 129SvJ, C57BL/6 and DBA/2 mouse lines.

Genetic constructs. The single exon gene encoding R9AP was amplified by PCR from mouse DNA and cloned into a modified baculovirus transfer vector pVL1392 (Skiba et al., 2001). The open reading frame of R9AP in this construct was preceded by a His_6 tag and a thrombin cleavage site. The constructs encoding R9AP fragments 1–217, 1–144, and 1–101 were generated by similar procedures, and they also contained N-terminal His_6 tags. The cloning of wild-type RGS9 and RGS9ΔDEP (amino acids 112–484) and the generation of recombinant baculoviruses were performed as described previously (Skiba et al., 2001).

Expression and purification of recombinant proteins. For protein expression, Sf-9 cells (2×10^7 cells/ml) were infected with recombinant baculoviruses and harvested 3 d after infection. The full-length R9AP was purified from the membrane fraction by sonicating Sf-9 cells in buffer A containing 50 mM NaH_2PO_4 (pH 8.0), 300 mM NaCl, and 10 mM imidazole, and sedimenting the membranes (30,000 × *g* for 30 min). R9AP was extracted from the pellet using buffer B (buffer A containing 1% lauryl sucrose). The extract was applied to Ni-NTA agarose beads (Qiagen, Hilden, Germany) and washed with buffer B containing 20 mM imidazole, and R9AP was eluted with buffer B containing 250 mM imidazole. The buffer was exchanged by gel filtration into buffer C: 25 mM Tris HCl (pH 7.8), 250 mM NaCl, 8 mM $MgCl_2$, and 1 mM DTT supplemented with 20% glycerol and stored at −80°C. The concentration of R9AP was determined spectrophotometrically using its theoretical molar extinction coefficient of $\epsilon_{280} = 13{,}260$. The soluble R9AP fragments 1–217, 1–144, and 1–101 were prepared according to the same protocol.

The wild-type RGS9 and RGS9ΔDEP (amino acids 112–484) were coexpressed with the long splice variant of Gβ5 in Sf-9 cells and purified as described by Skiba et al. (2001). Protein concentrations were determined spectrophotometrically using $\epsilon_{280} = 58{,}230$ for RGS9-Gβ5 and $\epsilon_{280} = 133{,}480$ for RGS9ΔDEP-Gβ5. To obtain membranes containing recombinant R9AP, Sf-9 cells were sonicated in buffer C, and crude cellular debris was sedimented for 15 min at 5000 × *g*. The membranes containing R9AP were then sedimented for 30 min at 30,000 × *g* and washed with buffer C. The amount of R9AP in these membranes was determined by quantitative Western blotting using purified R9AP as a standard. The membranes were stored at −80°C in buffer C containing 20% glycerol.

Purification of membranes and native proteins. Bovine ROS were isolated from frozen retinas as described by McDowell (1993). Urea-treated ROS lacking RGS9 activity (uROS) were prepared according to Nekrasova et al. (1997). Native R9AP present in the membranes after urea treatment was proteolyzed by Glu-C protease (protease V8; Sigma, St. Louis, MO) as described by Lishko et al. (2002). The V8-treated uROS membranes were sedimented for 30 min at 30,000 × *g* and washed twice with buffer C containing protease inhibitors. Rhodopsin concentration was determined spectrophotometrically using $\sigma_{500} = 40{,}000$ (Bownds et al., 1971). Transducin was purified from bovine ROS as described previously (Ting et al., 1993), and its concentration was determined on the basis of the maximum amount of rhodopsin-catalyzed GTPγS binding performed as described previously (Fung et al., 1981).

Antibody preparation and immunohistochemical analysis. The antibodies against mouse R9AP were obtained by immunizing rabbits with the 1–217 R9AP fragment. The serum was sequentially affinity-purified on the R9AP fragments 1–101, 1–144, and 1–217, yielding antibody fractions specific for the epitopes encoded by amino acids 1–101, 102–144, and 145–217, respectively. The antibodies against R9AP102–144 and rabbit antibodies against the C-terminal fragment of RGS9 (residues 226–484) were used for immunohistochemistry. For immunohistochemical detection of proteins in retina sections, eyes were fixed for 4 hr with paraformaldehyde (4% in PBS) at 4°C, cryoprotected with 30% sucrose in PBS at 4°C, and mounted in embedding medium (Tissue-Tek OCT Compound; Sakura, Torrance, CA). Frozen sections were obtained, rehydrated, blocked with PBT1 [PBS, 0.1% Triton X-100, 1% BSA (w/v), and 5% heat-inactivated goat serum] for 1 hr, incubated with primary antibody in PBT1 overnight at 4°C, washed four times with PBT2 (PBS, 0.1% Triton X-100, and 1% BSA), and incubated with fluorophore-conjugated secondary antibodies in PBT2 for 2 hr. After washing twice with PBT2 for 5 min and with PBS for 5 min, sections were mounted in PBS–glycerol and analyzed using a fluorescence microscope.

Serial tangential sectioning with Western blotting. This technique has been described in detail previously (Sokolov et al., 2002). Briefly, 2 mm round patches of mouse retinas were flat mounted between two glass slides separated by two 0.5-mm-thick spacers and frozen on dry ice. The slide with the vitreal side of retina attached was mounted on a cryomicrotome specimen holder, sequential 5 μm tangential retinal sections were obtained, and each section was collected in 50 μl of SDS-PAGE sample buffer. Proteins in each sample were analyzed by Western blotting using the following antibodies: rabbit antibody against R9AP102–144 fragment (see above); sheep anti-RGS9c antibody and rabbit anti-Gβ5 NT_L antibody described previously (Makino et al., 1999); A-6431 antibody (Molecular Probes, Eugene, OR) against cytochrome oxidase subunit IV (CoxIV); and 4D2 monoclonal antibody against rhodopsin (a gift from R. Molday, University of British Columbia, Vancouver, Canada). Band densities were quantified using the Personal Densitometer SI (Molecular Dynamics, Sunnyvale, CA).

GTPase assays. Multiple turnover assays of transducin GTPase activity were conducted as described previously (Skiba et al., 2000). In these assays, rhodopsin required for the GDP–GTP exchange on transducin was provided within uROS treated with protease V8 to inactivate endogenous RGS9 and R9AP. The reaction was conducted for 10 sec in 30 μl aliquots containing 200 μM [γ-^{32}P]GTP (~10^5 dpm/sample), 40 μM rhodopsin, 20 μM transducin, Sf-9 membranes containing 2 μM R9AP

Table 1. Electrophysiological comparison of DEP-less, RGS9 knock-out, and wild-type rods

	Dark current (pA)	Elementary amplitude (pA)	Dim flash recovery τ_{rec} (sec)	Bright flash τ_{dom} (sec)	I_o ($\phi/\mu m^2$)
RGS9 KO	10.8 ± 0.9 (12)	0.65 ± 0.12 (8)	2.66 ± 0.36 (9)	11.6 ± 0.3 (6)	45.8 ± 5.5 (10)
DEP-less	12.6 ± 1.0 (11)	0.49 ± 0.05 (9)	2.11 ± 0.20 (10)	10.7 ± 0.6 (7)	47.9 ± 8.4 (7)
WT	12.2 ± 0.7 (17)	0.56 ± 0.07 (16)	0.27 ± 0.02 (16)	0.37 ± 0.03 (13)	53.5 ± 4.8 (16)

I_o, Flash strength that elicited a half-maximal response. Error indicates SEM; number of rods is given in parentheses. KO, Knock-out; WT, wild type.

(R9AP), and 50 μM γ-subunit of cGMP phosphodiesterase 63–87 peptide (PDEγ_{63-87}) (added to maximize the efficiency of RGS9–transducin interactions) (Skiba et al., 2000). Control experiments indicated the following: the membranes from Sf-9 cells not expressing R9AP did not influence the activity of RGS9; the treatment of membranes containing R9AP with protease V8 completely abolished their ability to potentiate the activity of RGS9; the membranes containing R9AP did not influence the GTPase activity of transducin in the absence of RGS9; and the concentrations of GTP, transducin, and PDEγ_{63-87} were saturating.

Suction electrode recordings. Mice were housed in a 12 hr light/dark cycle overnight before an experiment. Under infrared light, animals were anesthetized and killed, and the retinas were removed and stored in L15 solution with 10 mM glucose and 0.1 mg/ml BSA on ice. Small pieces of retina were placed in the recording chamber and perfused with bicarbonate-buffered Locke's solution, bubbled with 95% O_2–5% CO_2, and warmed to 35–37°C, pH 7.4. Responses to flashes were recorded from individual dark-adapted rods using suction electrodes as described previously (Krispel et al., 2003). Briefly, individual mouse rods were drawn into a glass electrode containing the following (in mM): 140 NaCl, 3.6 KCl, 2.4 $MgCl_2$, 1.2 $CaCl_2$, 3 HEPES, 0.2 EDTA, and 10 glucose, pH 7.4. The bath and suction electrodes were connected to calomel half-cells by agar bridges, and the bath voltage was maintained at ground potential by an active feedback circuit. The rod membrane current was amplified (Axopatch 1B; Axon Instruments, Union City, CA) and filtered at 20 Hz with an eight-pole Bessel filter. Data was digitized continuously at 200 Hz using NiDAQ (National Instruments, Austin, TX) for IgorPro (WaveMetrics, Lake Oswego, OR). Tissue in the chamber was presented with 10 msec flashes of 500 nm light of calibrated intensity (United Detector Technology, Baltimore, MD).

The average response to a large number (>30) of flashes was considered to be in the linear range if its mean amplitude was <20% of the maximal response amplitude. These dim flash responses were used to estimate the form of the single photon response using the "variance to mean" method as described previously (Mendez et al., 2000). Integration time was used as a measure of the duration of the incremental flash response and is defined as the time integral of the average linear response divided by its peak amplitude (Baylor and Hodgkin, 1973). The time that a bright flash response remained in saturation was calculated as the time interval between the midpoint of the flash and the time at which the current recovered by 10%. The time constant of recovery for saturating flashes (τ_{dom}) (Table 1) was determined by regression analysis of the plot of the time in saturation versus the natural log of the flash strength in photons per square micrometer (Pepperberg et al., 1992).

Results

Generation and characterization of the mouse expressing RGS9 mutant lacking the DEP domain

The deletion of the DEP domain abolishes RGS9 interactions with R9AP *in vitro* (Lishko et al., 2002; Hu et al., 2003) but does not prevent RGS9 from forming a soluble, catalytically active complex with Gβ5 (He et al., 2000; Skiba et al., 2001). These properties of RGS9 enabled us to address the role of the DEP domain in subcellular targeting of RGS9 *in vivo* by using a transgenic mouse in which RGS9 was replaced by its mutant lacking the DEP domain (RGS9ΔDEP) (for the domain composition of the RGS9-Gβ5 complex, see Fig. 1*A*).

The RGS9ΔDEP transgene was specifically expressed in rods under the control of the rhodopsin upstream regulatory region

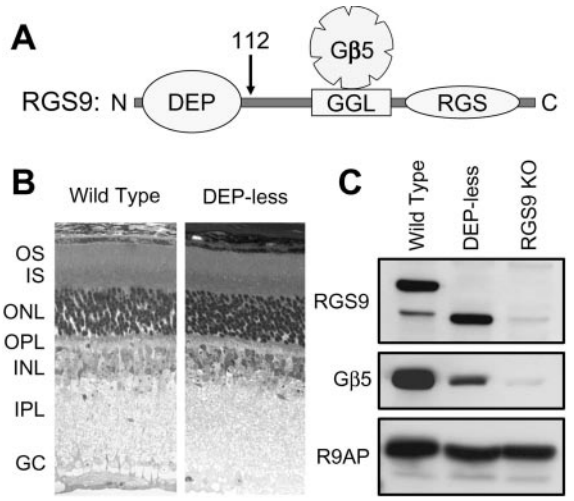

Figure 1. Characterization of the retinas from DEP-less mice. *A*, Domain composition of the RGS9-Gβ5 complex. GGL, G-protein γ-subunit-like domain; RGS, RGS homology domain. The arrow marks the point of the DEP domain deletion in RGS9ΔDEP. *B*. Cross-sections (1 μm) of the retinas from 6-month-old wild-type and DEP-less mice stained by toluidine blue. OS, Outer segment layer; IS, inner segment layer; ONL, outer nuclear layer; OPL, outer plexiform layer; INL, inner nuclear layer; IPL, inner plexiform layer; GC, ganglion cell layer. *C*, Western blot analysis of RGS9, Gβ5, and R9AP in the retinas of wild-type, DEP-less, and RGS9 knock-out (KO) mice. Each lane contained 15 pmol of rhodopsin. The lower band of the RGS9 staining of wild-type animals' retinas represents a C-terminal proteolytic fragment of RGS9 present in most RGS9 preparations (He et al., 2000; Lishko et al., 2002).

(Lem et al., 1991) (see Materials and Methods). Animals carrying the RGS9ΔDEP transgene were crossed with RGS9 knock-outs (Chen et al., 2000), and a line expressing RGS9ΔDEP on the RGS9 knock-out background was established. We call these animals "DEP-less mice." These mice displayed normal retinal morphology up to 6 months of age (Fig. 1*B*). The total amount of rhodopsin in DEP-less retinas was also normal (466 ± 57 pmol per retina vs 470 ± 110 pmol per retina in wild-type mice; mean ± SEM; $n = 4$). The level of RGS9ΔDEP expression in DEP-less mice was similar to the RGS9 expression level in wild-type mice (Fig. 1*C*). Approximately one-half of RGS9ΔDEP was extractable from the retinas of DEP-less mice, whereas no detectable RGS9 could be extracted from the retinas of wild-type animals under nondenaturing conditions (data not shown). The expression of RGS9ΔDEP also resulted in a partial restoration of Gβ5 (Fig. 1*C*), which was absent in RGS9 knock-out animals (Fig. 1*C*) (Chen et al., 2000). The amount of R9AP in DEP-less mice was reduced by ~30% compared with that in wild-type mice and was essentially the same as in RGS9 knock-outs (Fig. 1*C*).

Deletion of the DEP domain alters the subcellular localization of RGS9

We first analyzed the subcellular distribution of RGS9 and RGS9ΔDEP in rods of wild-type and DEP-less mice, respectively, by immunostaining retinal cross-sections (Fig. 2, top panel). In agreement with previous reports (Cowan et al., 1998; Zhang et al.,

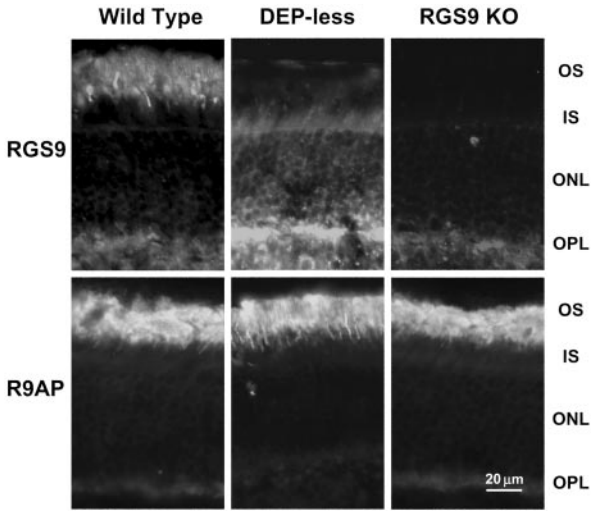

Figure 2. Immunohistochemical analysis of RGS9 (top panel) and R9AP (bottom panel) distribution in rods of wild-type, DEP-less, and RGS9 knock-out (KO) mice. For details, see Materials and Methods. For abbreviations of the retina layers, see Figure 1 legend.

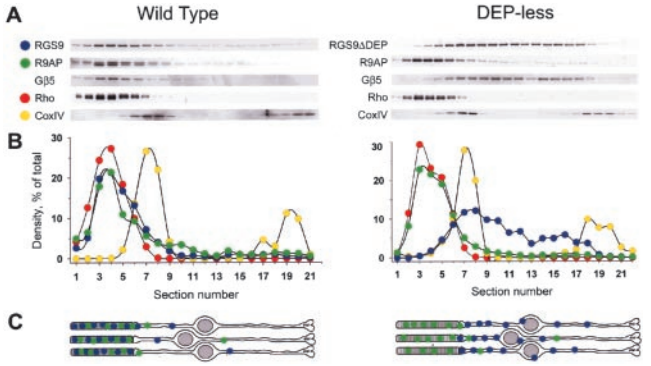

Figure 3. Quantitative analysis of RGS9 and R9AP distribution in rods of wild-type and DEP-less mice by cryosectioning with Western blotting. *A*, Western blots of RGS9, R9AP, Gβ5, and two marker proteins, rhodopsin (Rho) and CoxIV. *B*, Densitometric profiles of the Western blots from *A* in which the densities of individual bands for RGS9, R9AP, rhodopsin, and CoxIV are expressed as a percentage of the total density of all bands representing each individual protein on the blot. *C*, A drawing illustrating the distribution of RGS9 and R9AP at their respective locations in rods of wild-type and DEP-less mice. The data are taken from one of three similar experiments.

2003), RGS9 staining in photoreceptors of wild-type mice was restricted to the outer segments (Fig. 2, top panel). However, almost no RGS9ΔDEP staining was present in the outer segments of DEP-less mice. Instead, staining was observed throughout the rest of the photoreceptor cells, from the inner segments to the synaptic terminals. Unlike RGS9, the distribution of R9AP in photoreceptors of DEP-less mice was similar to that of wild-type animals, as well as RGS9 knock-outs (Fig. 2, bottom panel). In all cases, most of the R9AP immunostaining signal was observed in the outer segments.

We next addressed the distribution of RGS9ΔDEP in photoreceptors by using a quantitative technique of serial tangential sectioning with Western blotting developed recently in one of our laboratories (Sokolov et al., 2002). The retinas were rapidly extracted from mouse eyes, flat mounted, frozen, and serially sectioned so that each section yielded one progressive 5-μm-thick slice of the photoreceptor layer. The proteins in each section were then analyzed by Western blotting, and the colocalization of proteins of interest with protein markers confined to various subcellular compartments was assessed. We used rhodopsin as the outer segment marker and CoxIV as the mitochondrial marker predominantly present in the ellipsoid part of the inner segments and synaptic terminals. The distribution of at least 90% of RGS9 in serial sections from wild-type mice coincided with the distribution of rhodopsin, indicating that RGS9 is localized exclusively to rod outer segments (Fig. 3). In contrast, practically no RGS9ΔDEP was present in the outer segments of DEP-less mice, with almost all distributed throughout the entire length of the photoreceptor layer. Only trace amounts of RGS9ΔDEP were identified in the outer segment sections completely free of the inner segment contamination, as judged by the absence of cytochrome oxidase. The distribution of Gβ5 throughout the sections coincided with the distribution of RGS9 or RGS9ΔDEP.

Using the same blots, we examined the subcellular distribution of R9AP (Fig. 3). In agreement with immunohistochemical data, most R9AP in both wild-type and DEP-less mice was localized to rod outer segments. In some sections, R9AP immunostaining revealed two close bands. We found that the upper band represented phosphorylated R9AP because treatment of the samples with alkaline phosphatase eliminated the upper band and increased staining of the lower band (data not shown). A small fraction of R9AP was also present in the rest of the cell, as noted previously (Hu and Wensel, 2002). However, the amount of R9AP present in sections not containing the outer segments (judged by the absence of rhodopsin) was <20% of its total amount in both wild-type and DEP-less mice.

Additional experiments revealed that the subcellular distribution of all of the proteins analyzed in this study was the same in dark- and light-adapted animals (data not shown). In summary, our data show that the removal of the DEP domain from RGS9 resulted in a major cellular mislocalization of RGS9 and Gβ5 but not R9AP, indicating that the DEP domain interaction with R9AP is crucial for RGS9 targeting to rod outer segments.

Electrophysiological properties of the rods from DEP-less mice

Additional evidence that no functional activity of RGS9 was present in the outer segments of DEP-less mice was obtained by comparing photoresponses recorded from rods of DEP-less, wild-type, and RGS9 knock-out mice. Previous study indicated that RGS9 knock-out rods have slowed GTP hydrolysis by transducin, which causes slow rate of recovery of the light response (Chen et al., 2000). The data from Figure 4 and Table 1 indicate that the photoresponses from rods of the DEP-less mice were essentially identical to those from rods of the RGS9 knock-out mice. In both cases, the final falling phase of the single photon response recovered along an exponential time course with a time constant (τ_{rec}) of ~2 sec, approximately an order of magnitude slower than that measured for wild-type responses (Fig. 4*A*, Table 1). The differences between the responses of wild-type and those of RGS9 knock-out and DEP-less rods were limited to the final recovery phases; general measures of photoreceptor viability, including the dark currents and sensitivities (I_o), were practically indistinguishable (Fig. 4*B*, Table 1). As described previously (Chen et al., 2000; Krispel et al., 2003), the recovery of rods lacking RGS9 slowed as the flash strength increased (Fig. 4*B*). DEP-less rods also showed this same behavior, yielding a time constant of recovery for saturating flashes that was indistinguishable from RGS9 knock-out rods (τ_{dom} ~11 sec) (Table 1). The similarity of rates of recovery of RGS9 knock-out and DEP-less responses across a wide range of flash strengths indicated that

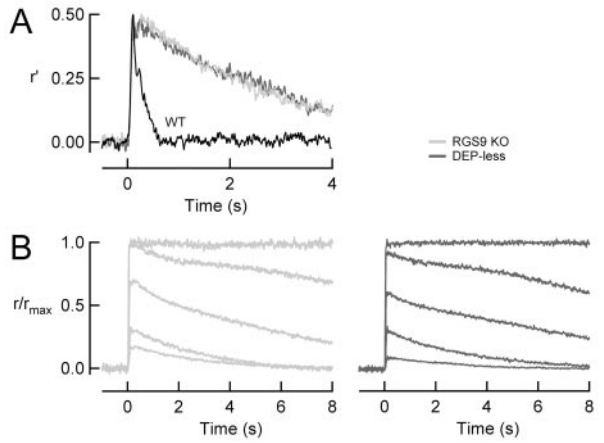

Figure 4. Flash responses of DEP-less rods resemble those of RGS9 knock-out rods. *A*, Representative mean single photon responses from wild-type, RGS9 knock-out (KO), and DEP-less rods. Amplitudes have been normalized to the mean DEP-less single photon response amplitude (0.49 pA) to aid comparison of recovery kinetics. *B*, Families of responses to increasing flash strengths from RGS9 knock-out (red) and DEP-less (blue) rods. Each trace is the average of 2 (bright) to 30 (dim) flashes. Dark currents were 9.2 pA (RGS9 knock-out) and 13.9 pA (DEP-less). Flash strengths ranged from 5.3 to 718 photons/μm^2 by factors of 4 (DEP-less) and 9.6 and from 18.1 to 733 photons/μm^2 by factors of 4 (RGS9 knock-out).

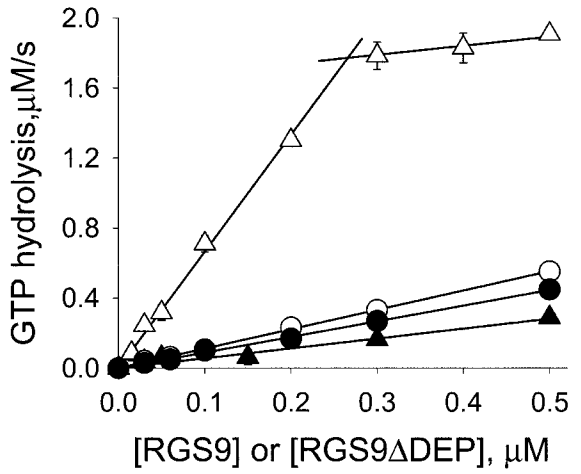

Figure 5. The stimulation of RGS9 ability to activate transducin GTPase is abolished by deletion of the DEP domain. Multiple turnover transducin GTPase assays were performed as described in Materials and Methods. The basal GTPase activity of transducin measured without RGS9 or RGS9ΔDEP was subtracted from the values measured with RGS9, and the resulting values were plotted on the graph. Triangles represent the measurements conducted with full-length RGS9; circles represent the measurements conducted with RGS9ΔDEP; filled symbols represent the measurements conducted in the absence of R9AP; and open symbols represent the measurements conducted in the presence of R9AP. The data for the three bottom plots were fitted by straight lines, whereas the data obtained with RGS9 in the presence of R9AP were fitted by two straight lines (for the values of the rates, see Results). Data were averaged from three independent experiments; error bars represent SEM.

there was no significant functional activity of RGS9 present in the outer segments of DEP-less mice.

Deletion of the DEP domain abolishes the regulation of RGS9 activity by R9AP

Previous reports demonstrated that RGS9 binding to R9AP results in significant potentiation of its ability to stimulate transducin GTPase activity (Lishko et al., 2002; Hu et al., 2003). We therefore analyzed the consequences of the DEP domain deletion for the regulation of RGS9 GTPase activity by R9AP by conducting multiple turnover transducin GTPase assays. With full-length RGS9 assayed in the absence of R9AP, the rate of GTP hydrolysis increased linearly with RGS9 concentration, corresponding to a relatively low level of RGS9 activity of 0.54 ± 0.05 mol GTP/mol RGS9/sec (Fig. 5). When R9AP was added, the increase in the GTP hydrolysis rate increased biphasically with RGS9 concentration. The slope of the initial steep phase was 6.5 ± 0.2 mol GTP/mol RGS9/sec, or ~12-fold higher than in the absence of R9AP, whereas the slope of the subsequent phase was 0.62 ± 0.30 mol GTP/mol RGS9/sec, essentially the same as that in the absence of R9AP. Similar biphasic plots were documented in previous studies (Lishko et al., 2002; Hu et al., 2003) in which the transition point reflected the maximal amount of R9AP available for binding to RGS9 in the assays. Therefore, we conclude that the stimulatory effect of recombinant R9AP on the ability of RGS9 to activate transducin GTPase was ~12-fold and that the transition point corresponded to the amount of functionally active R9AP in the preparation. It is interesting to note that the 12-fold effect observed in our experiments is larger than the approximate fourfold effect observed with recombinant R9AP by others (Hu et al., 2003). However, it is lower than the ~70-fold effect observed with native photoreceptor membranes containing endogenous R9AP (Lishko et al., 2002), leaving a possibility that the regulation of RGS9 activity in photoreceptors remains not completely understood.

In contrast to full-length RGS9, the activity of RGS9ΔDEP was not regulated by R9AP, further supporting the role of the DEP domain in RGS9–R9AP interactions (Fig. 5). The basal activity of RGS9ΔDEP in the absence of R9AP was approximately twofold higher than that of RGS9. However, the addition of R9AP-containing membranes to RGS9ΔDEP neither caused a reliable increase in the rate of GTP hydrolysis (0.9 ± 0.1 vs 1.1 ± 0.1 mol GTP/mol RGS9/sec) nor induced a biphasic behavior of the plot. We therefore conclude that all of the stimulation of RGS9 activity by R9AP is mediated via interactions with the DEP domain.

Discussion

The role of the DEP domain in the functioning of RGS9

The principal observation of this study is that the DEP domain of RGS9 is essential for RGS9 delivery to rod outer segments. Our quantitative analysis shows that, although the majority of wild-type RGS9 is localized to rod outer segments, its mutant lacking the DEP domain is excluded from the outer segments. This result cannot be explained simply by the lack of ability by RGS9ΔDEP to bind to its docking sites at the outer segment discs provided by R9AP, which would be expected to result in even distribution of RGS9ΔDEP throughout the cytoplasm of the entire rod cell but not in its absence from the outer segments. We therefore think that the most plausible explanation for the absence of RGS9ΔDEP in rod outer segments is that RGS9 binding to R9AP is a prerequisite step in directing RGS9 subcellular localization and that this interaction must occur before the entrance of these proteins to the outer segments. We think it is unlikely that the mislocalization of RGS9ΔDEP could only be a result of its misfolding because the complex of RGS9ΔDEP with Gβ5 is both soluble and catalytically active in the absence of R9AP (Fig. 5). In this context, the relatively low levels of Gβ5 in the rods of DEP-less mice could be explained by proteolytic degradation of Gβ5 in the cellular compartment in which it is not normally present.

This novel and perhaps most crucial function of the DEP domain of RGS9 is complemented by two other functions revealed in previous studies. The first is to keep RGS9 bound to the disc membranes of rod outer segments, which results in potentiation

of the ability by RGS9 to activate transducin GTPase via the interaction with R9AP (Lishko et al., 2002; Hu et al., 2003) (Fig. 5). The second is to regulate RGS9 substrate recognition specificity. The deletion of the DEP domain results in the reduction of the ability of RGS9 to interact selectively with transducin bound to its effector, the γ-subunit of cGMP phosphodiesterase, rather than with free activated transducin (Skiba et al., 2001). This latter property of RGS9 is important for terminating the G-protein signal after, but not before, transducin activates phosphodiesterase during the course of the photoresponse (for review, see Arshavsky et al., 2002).

Hypothesis: targeting of signaling proteins to specific intracellular compartments is a general function of DEP domains

In this study, we obtained direct *in vivo* evidence that a DEP domain can govern subcellular targeting of a signaling protein. Is it possible that DEP domains present in many other signaling proteins serve the same function? This possibility is supported by several recent results obtained with other DEP-containing proteins. As such, the binding of Disheveled protein (a component of the Wingless signaling pathway) to cell plasma membrane caused by overexpression of a Frizzled receptor in embryonic ectoderm cells was specifically abolished by the deletion of the C-terminal DEP domain of Disheveled (Axelrod et al., 1998). Similarly, deleting the DEP domain from Epac (the cAMP-dependent guanine nucleotide exchange factor for small GTP-binding proteins of the Rap family) abolished the ability of Epac to associate with the nuclear membrane during expression in cell culture (de Rooij et al., 2000; Qiao et al., 2002). In *Saccharomyces cerevisiae*, the RGS9 homolog *Sst*II undergoes proteolytic digestion, yielding a fragment containing the RGS homology domain and another fragment containing the DEP domain. This proteolysis was followed by association of the DEP-containing fragment with the microsomal membranes and release of the RGS-containing fragment to the cytoplasm (Hoffman et al., 2000). In *Caenorhabditis elegans*, transgenic expression of the DEP domain-containing fragment of the RGS protein EGL-10 (for regulator of serotonin-stimulated egg laying) determined the solubility of another EGL-10 fragment containing the rest of the molecule (Patikoglou and Koelle, 2002). The authors interpreted these data as an indication for the DEP-directed membrane association of EGL-10.

These four examples, taken from very diverse signaling cascades, complement our direct data and support our hypothesis that targeting signaling proteins to specific membranous subcellular compartments is likely to be a general function of DEP domains. Is it possible that this targeting occurs through a common pattern of protein–protein interactions? A clue for answering this question might be provided by the similarity between R9AP and proteins of the SNARE (soluble *N*-ethylmaleimide-sensitive factor attachment protein receptor) family involved in vesicular trafficking and membrane fusion (Fig. 6). SNAREs are membrane-associated proteins containing either transmembrane domains (such as syntaxins and synaptobrevins) or palmitoylated cysteines (such as SNAP-25) (for review, see Harbury, 1998; Chen and Scheller, 2001). The most general structural feature of SNAREs is that they have a conserved domain containing a coiled-coil motif, which is responsible for the formation of hetero-oligomeric complexes among different SNARE proteins. This domain has either an arginine or a glutamine residue at a highly conserved position at the core of the coiled coil, providing the basis for classification as R or Q SNAREs, respectively (Fasshauer et al., 1998) (Fig. 6). Some SNAREs, such as syntaxin,

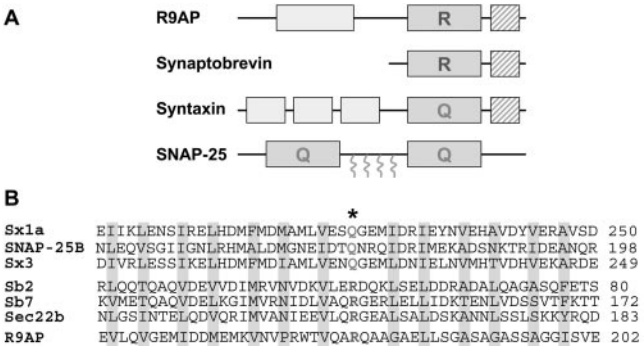

Figure 6. R9AP shares structural similarities with SNARE protein family members. *A*, Schematic representation of R9AP domain composition in comparison with three canonical SNARE proteins. Hashed boxes represent transmembrane regions; dark boxes represent conservative domains participating in SNARE complex formation; light boxes represent domains with predicted coiled-coil folds; and wavy lines represent palmitoyl groups responsible for membrane attachment of SNAP-25. *B*, Sequence alignment of the coiled-coil regions involved in the formation of the SNARE complexes with the corresponding region of mouse R9AP. The position of the conserved ionic layer is marked with an asterisk. Gray boxes mark the conserved positions of the heptad repeats. Sx1a, Rat syntaxin 1a (GenBank accession number P32851); SNAP-25B, rat SNAP-25B (GenBank accession number P13795); Sx3, rat syntaxin 3 (GenBank accession number Q08849); sb2, rat synaptobrevin 2 (GenBank accession number M24105); sb7, mouse synaptobrevin 7 (GenBank accession number X96737); Sec22b, mouse vesicle trafficking protein Sec22b (GenBank accession number U91538).

may contain additional domains forming coiled coils. As in SNARE proteins, R9AP contains a characteristic coiled-coil region immediately preceding the C-terminal transmembrane segment. Our analysis indicates that R9AP may be considered an R-SNARE on the basis of the presence of an arginine at the conserved position (Fig. 6). R9AP also contains an N-terminal domain predicted to form coiled coils, similar to the SNARE protein syntaxin. Because R9AP has not yet been shown to interact with other SNAREs or to participate in vesicular transport, we classify R9AP as a SNARE-like protein.

Significant similarities between R9AP and SNARE proteins open the possibility that the interaction of R9AP with RGS9 may reflect a more general pattern of DEP–SNARE interactions. Evidence in support of this hypothesis was obtained in a recent study of another DEP-containing RGS protein, RGS7 (Hunt et al., 2003). The authors identified a SNARE-associated protein, snapin, as the RGS7 interacting partner and showed that snapin can bind to an RGS7 fragment containing the DEP domain. Additional evidence for a similar interaction has been revealed in a yeast two-hybrid screen with the DEP domain of *Sst*II, in which two syntaxin homologs were identified as its potential binding partners (Burchett et al., 2002).

The hypothesis that DEP–SNARE interactions are crucial for intracellular protein targeting brings a new twist to studies of molecular mechanisms underlying membrane targeting of signaling proteins. Most of the previously described mechanisms are based on the recognition of specific lipid components by specialized protein domains, such as PX domains interacting with membrane phosphoinositides (for review, see Sato et al., 2001). The significance of our hypothesis lies in its three major predictions. First, DEP domains should be considered as "passports" that allow signaling proteins to reach specific intracellular compartments. Second, this targeting is predicted to be mediated by members of the SNARE protein superfamily, which would expand the spectrum of the function of the SNARE proteins. Third, DEP-containing signaling proteins may be involved in the regu-

lation of conventional SNARE functions, such as synaptic transmission and other forms of exocytosis.

References

Arshavsky VY, Lamb TD, Pugh Jr EN (2002) G proteins and phototransduction. Annu Rev Physiol 64:153–187.

Axelrod JD, Miller JR, Shulman JM, Moon RT, Perrimon N (1998) Differential recruitment of Dishevelled provides signaling specificity in the planar cell polarity and Wingless signaling pathways. Genes Dev 12:2610–2622.

Baylor DA, Hodgkin AL (1973) Detection and resolution of visual stimuli by turtle photoreceptors. J Physiol (Lond) 234:163–198.

Bownds D, Gordon-Walker A, Gaide-Huguenin A-C, Robinson W (1971) Characterization and analysis of frog photoreceptor membranes. J Gen Physiol 58:225–237.

Burchett SA (2000) Regulators of G protein signaling: a bestiary of modular protein binding domains. J Neurochem 75:1335–1351.

Burchett SA, Flanary P, Aston C, Jiang L, Young KH, Uetz P, Fields S, Dohlman HG (2002) Regulation of stress response signaling by the N-terminal dishevelled/EGL-10/pleckstrin domain of Sst2, a regulator of G protein signaling in Saccharomyces cerevisiae. J Biol Chem 277:22156–22167.

Chen CK, Burns ME, He W, Wensel TG, Baylor DA, Simon MI (2000) Slowed recovery of rod photoresponse in mice lacking the GTPase accelerating protein RGS9–1. Nature 403:557–560.

Chen YA, Scheller RH (2001) SNARE-mediated membrane fusion. Nat Rev Mol Cell Biol 2:98–106.

Cowan CW, Fariss RN, Sokal I, Palczewski K, Wensel TG (1998) High expression levels in cones of RGS9, the predominant GTPase accelerating protein of rods. Proc Natl Acad Sci USA 95:5351–5356.

Cowan CW, He W, Wensel TG (2000) RGS proteins: lessons from the RGS9 subfamily. Prog Nucleic Acid Res Mol Biol 65:341–359.

de Rooij J, Rehmann H, van Triest M, Cool RH, Wittinghofer A, Bos JL (2000) Mechanism of regulation of the Epac family of cAMP-dependent RapGEFs. J Biol Chem 275:20829–20836.

Fasshauer D, Sutton RB, Brunger AT, Jahn R (1998) Conserved structural features of the synaptic fusion complex: SNARE proteins reclassified as Q- and R-SNAREs. Proc Natl Acad Sci USA 95:15781–15786.

Fung BBK, Hurley JB, Stryer L (1981) Flow of information in the light-triggered cyclic nucleotide cascade of vision. Proc Natl Acad Sci USA 78:152–156.

Harbury PA (1998) Springs and zippers: coiled coils in SNARE-mediated membrane fusion. Structure 6:1487–1491.

He W, Cowan CW, Wensel TG (1998) RGS9, a GTPase accelerator for phototransduction. Neuron 20:95–102.

He W, Lu LS, Zhang X, El Hodiri HM, Chen CK, Slep KC, Simon MI, Jamrich M, Wensel TG (2000) Modules in the photoreceptor RGS9–1·$G_{\beta 5L}$ GTPase-accelerating protein complex control effector coupling, GTPase acceleration, protein folding, and stability. J Biol Chem 275:37093–37100.

Hoffman GA, Garrison TR, Dohlman HG (2000) Endoproteolytic processing of Sst2, a multidomain regulator of G protein signaling in yeast. J Biol Chem 275:37533–37541.

Hu G, Wensel TG (2002) R9AP, a membrane anchor for the photoreceptor GTPase accelerating protein, RGS9–1. Proc Natl Acad Sci USA 99:9755–9760.

Hu G, Zhang Z, Wensel TG (2003) Activation of RGS9–1 GTPase acceleration by its membrane anchor, R9AP. J Biol Chem 278:14550–14554.

Hunt RA, Edris W, Chanda PK, Nieuwenhuijsen B, Young KH (2003) Snapin interacts with the N-terminus of regulator of G protein signaling 7. Biochem Biophys Res Commun 303:594–599.

Krispel CM, Chen C-K, Simon MI, Burns ME (2003) Prolonged photoresponses and defective adaptation in rods of $G5^{-/-}$ mice. J Neurosci 23:6965–6971.

Lem J, Applebury ML, Falk JD, Flannery JG, Simon MI (1991) Tissue-specific and developmental regulation of rod opsin chimeric genes in transgenic mice. Neuron 6:201–210.

Lishko PV, Martemyanov KA, Hopp JA, Arshavsky VY (2002) Specific binding of RGS9-Gβ5L to protein anchor in photoreceptor membranes greatly enhances its catalytic activity. J Biol Chem 277:24376–24381.

Makino ER, Handy JW, Li TS, Arshavsky VY (1999) The GTPase activating factor for transducin in rod photoreceptors is the complex between RGS9 and type 5 G protein β subunit. Proc Natl Acad Sci USA 96:1947–1952.

McDowell JH (1993) Preparing rod outer segment membranes, regenerating rhodopsin, and determining rhodopsin concentration. Methods Neurosci 15:123–130.

Mendez A, Burns ME, Roca A, Lem J, Wu LW, Simon MI, Baylor DA, Chen J (2000) Rapid and reproducible deactivation of rhodopsin requires multiple phosphorylation sites. Neuron 28:153–164.

Nekrasova ER, Berman DM, Rustandi RR, Hamm HE, Gilman AG, Arshavsky VY (1997) Activation of transducin guanosine triphosphatase by two proteins of the RGS family. Biochemistry 36:7638–7643.

Patikoglou GA, Koelle MR (2002) An N-terminal region of *Caenorhabditis elegans* RGS proteins EGL-10 and EAT-16 directs inhibition of $G\alpha_o$ versus $G\alpha_q$ signaling. J Biol Chem 277:47004–47013.

Pepperberg DR, Cornwall MC, Kahlert M, Hofmann KP, Jin J, Jones GJ, Ripps H (1992) Light-dependent delay in the falling phase of the retinal rod photoresponse. Vis Neurosci 8:9–18.

Ponting CP, Bork P (1996) Pleckstrin's repeat performance: a novel domain in G-protein signaling? Trends Biochem Sci 21:245–246.

Qiao J, Mei FC, Popov VL, Vergara LA, Cheng X (2002) Cell cycle-dependent subcellular localization of exchange factor directly activated by cAMP. J Biol Chem 277:26581–26586.

Sato TK, Overduin M, Emr SD (2001) Location, location, location: membrane targeting directed by PX domains. Science 294:1881–1885.

Skiba NP, Hopp JA, Arshavsky VY (2000) The effector enzyme regulates the duration of G protein signaling in vertebrate photoreceptors by increasing the affinity between transducin and RGS protein. J Biol Chem 275:32716–32720.

Skiba NP, Martemyanov KA, Elfenbein A, Hopp JA, Bohm A, Simonds WF, Arshavsky VY (2001) RGS9-Gβ5 substrate selectivity in photoreceptors—opposing effects of constituent domains yield high affinity of RGS interaction with the G protein-effector complex. J Biol Chem 276:37365–37372.

Sokol S (2000) A role for Wnts in morphogenesis and tissue polarity. Nat Cell Biol 2:E124–E125.

Sokolov M, Lyubarsky AL, Strissel KJ, Savchenko AB, Govardovskii VI, Pugh Jr EN, Arshavsky VY (2002) Massive light-driven translocation of transducin between the two major compartments of rod cells: a novel mechanism of light adaptation. Neuron 34:95–106.

Sung CH, Tai AW (2000) Rhodopsin trafficking and its role in retinal dystrophies. Int Rev Cytol 195:215–267.

Ting TD, Goldin SB, Ho Y-K (1993) Purification and characterization of bovine transducin and its subunits. Methods Neurosci 15:180–195.

Tsang SH, Burns ME, Calvert PD, Gouras P, Baylor DA, Goff SP, Arshavsky VY (1998) Role for the target enzyme in deactivation of photoreceptor G protein in vivo. Science 282:117–121.

Williams DS (2002) Transport to the photoreceptor outer segment by myosin VIIa and kinesin II. Vision Res 42:455–462.

Zhang X, Wensel TG, Kraft TW (2003) GTPase regulators and photoresponses in cones of the eastern chipmunk. J Neurosci 23:1287–1297.-